Brain, Behavior, & Immunity - Health 42 (2024) 100891

Contents lists available at ScienceDirect

Brain, Behavior, & Immunity - Health

journal homepage: www.editorialmanager.com/bbih/default.aspx

Prophylactic clemastine treatment improves influenza A virus-induced cognitive dysfunction in mice

J.D. Tingling [a,1], S.A. Krauklis [b,1], P.L. Haak [a], R. Carr [a], A.Y. Louie [c], R.W. Johnson [a,b,c], A.J. Steelman [a,b,c,d,*]

[a] Department of Animal Sciences, University of Illinois at Urbana-Champaign, 1201 W. Gregory Dr., Urbana, IL, 61801, USA
[b] Division of Nutritional Sciences, University of Illinois at Urbana-Champaign, 1201 W. Gregory Dr., Urbana, IL, 61801, USA
[c] Neuroscience Program, University of Illinois at Urbana-Champaign, USA
[d] Carl R. Woese Institute for Genomic Biology, University of Illinois at Urbana-Champaign, 1206 West Gregory Dr. Urbana, IL, 61801, USA

ARTICLE INFO

Keywords:
Respiratory virus infection
Cognitive impairment
Oligodendrocyte
Clemastine

ABSTRACT

Respiratory infection by influenza A virus (IAV) is known to cause systemic inflammation, neuroinflammation, and cognitive impairment. We previously found that experimental infection with IAV affected oligodendrocyte homeostasis, which was associated with altered expression of genes involved in myelin maintenance as well as the lipidome. In this study, we sought to determine if clemastine, an antihistamine with myelin promoting properties, could reverse the effects of IAV on oligodendrocyte (OL) specific genes, as well as mitigate infection-induced cognitive impairment. Male and female C57BL/6J mice were randomized into experimental groups based on clemastine treatment, infection, and sex. Treatment with vehicle or clemastine (10 mg/kg/d) commenced seven days prior to inoculation with either saline or IAV and continued throughout the experiment. Body weight was measured throughout the infection. Spatial learning and memory were assessed by Morris water maze. Sickness behavior was assessed by measuring burrowing response. Immune cell responses were determined by flow cytometry, RT-qPCR, antigen recall assays and ELISA, and viral load assessed by RT-qPCR. Hippocampal levels of neuroinflammatory (*Tnf, Cdkn1a*) and myelin (*Plp1*, *Mag*, *Ugt8a*) genes were determined by RT-qPCR. Mice infected with IAV developed weight loss, impaired cognitive flexibility, reduced burrowing behavior, altered lung immune cell infiltration, increased circulating anti-viral IgM and IgG levels and increased T cell responses to IAV epitopes. Infection increased hippocampal levels of genes associated with neuroinflammation and decreased levels of genes involved in myelination. Clemastine treatment resulted in earlier recovery of weight loss in males and increased IgM levels for both sexes, but neither affected expression levels of *Tnf* or *Cdkn1a*, nor rescued changes to oligodendrocyte genes. However, treatment mitigated infection-induced neurocognitive impairment.

1. Introduction

Respiratory viral pathogens such as influenza A virus (IAV) and severe acute respiratory syndrome coronavirus (SARS-CoV)-2 remain both a national and global public health concern. For instance, IAV (Dawood et al., 2012) alone is responsible for ~3–5 million annual cases of severe illness, resulting in between 290 and 650K deaths worldwide (World Health Organization; Centers for Disease Control and Prevention). According to the World Health Organization, more than 770 million people have been infected by SARS-CoV-2, resulting in greater than 7 million deaths. While IAV and SARS-CoV-2 infections are associated with acute onset of respiratory distress, both are also capable of causing neurological sequelae including cognitive impairment (Volk et al., 2023; Thaweethai et al., 2023; Schlesinger et al., 1998). Neurological complications following IAV infection were first observed during the 1918 pandemic and have since manifested in patients of subsequent

Abbreviations: (COVID-19), Coronavirus induced disease 19; (Cdkn1a), Cyclin dependent kinase inhibitor 1A; (IAV), Influenza A virus; (Mag), Myelin associated glycoprotein; (Plp), Proteolipid protein; (SARS-CoV-2), Severe acute respiratory syndrome coronavirus 2; (Tnf), Tumor necrosis factor; (Ugt8a), UDP-galactose ceramide galatosyltranserase 8a.

* Corresponding author. Department of Animal Sciences, University of Illinois at Urbana-Champaign, 1201 W. Gregory Dr., Urbana, IL, 61801, USA.
E-mail address: asteelma@illinois.edu (A.J. Steelman).

[1] Co-first authors.

https://doi.org/10.1016/j.bbih.2024.100891
Received 24 January 2024; Received in revised form 20 September 2024; Accepted 5 October 2024
Available online 9 October 2024

pandemics. These complications range from short-term sequelae, such as altered mental status, to seriously debilitating clinical outcomes, such as increased risk for development of neurodegenerative disease, seizures or coma, with clear long-term morbidity and mortality (Ekstrand, 2012; Maurizi, 2010; Ravenholt and Foege, 1982; Jelliffe, 1919). As might be expected, neuropsychiatric complications have been reported following infection by neurotropic strains of IAV such as H5N1 strains, which are capable of gaining access to the central nervous system (CNS) by crossing the blood-brain barrier (Jang et al., 2009, 2012). However, these sequelae can also be present in patients infected by IAV strains that are non-neurotropic, such as H1N1 strains (Schlesinger et al., 1998; Ekstrand, 2012; Surana et al., 2011; Wang et al., 2010). Likewise, cognitive deficit is reportedly one of the main disabling symptoms in COVID-19 patients (Thaweethai et al., 2023; Graham et al., 2021; Xu et al., 2022). As such, an area of important scientific investigation continues to be the neuroinflammatory mechanisms that underlie neurological complications that are observed in association with respiratory virus infection.

Prior work has shown that aberrant activation of the peripheral innate immune system can lead to the increased production of pro-inflammatory cytokines within the brain, leading to neuropathology in specific areas, such as the hippocampus, the region of the brain responsible for spatial learning and memory (Heneka et al., 2014; Korte and Schmitz, 2016; Camara et al., 2015; Raison et al., 2006; Riazi et al., 2015; Thomson et al., 2014; Vitkovic et al., 2000; Jurgens et al., 2012; Hosseini et al., 2018). To date, research has been centered on examining the effect of respiratory infection on neuronal function, as these cells are a major driver of cognitive performance. Less research has addressed the involvement of glia, such as oligodendrocytes in this process. Oligodendrocytes are CNS resident cells that provide trophic and metabolic support for neurons (Fünfschilling et al., 2012; Oluich et al., 2012; Meyer et al., 2018; Chamberlain et al., 2021), but are most commonly associated with their production of myelin, the substance of white matter that is required for saltatory conduction. We previously found that experimental respiratory infection of adult mice with IAV alters oligodendrocyte homeostasis in a manner that was characterized by the suppression of oligodendrocyte specific gene transcription as well as alterations to the lipid profile of myelin itself. Transcriptional changes resulting from peripheral IAV infection occurred within the cerebellum, medial prefrontal cortex, and also the hippocampus and was concurrent with decreased protein expression within acutely isolated oligodendrocytes (Louie et al., 2023). This phenomenon is of particular interest since 1) experiments performed in mice have indicated that oligodendrocytes are essential for new memory formation (McKenzie et al., 2014; Pan et al., 2020; Steadman et al., 2020; Shimizu et al., 2023) and 2) a recent study has demonstrated that SARS-CoV-2 infection causes myelin loss in the hippocampus of mice, and may serve as a pathological mechanism for “COVID fog” (Fernandez-Castaneda et al., 2022). However, whether changes to oligodendrocyte functions by respiratory infection are linked to altered cognitive capacity is not yet known.

Clemastine fumarate (i.e. clemastine) is a United States Food and Drug Administration (FDA) approved first-generation anti-histamine drug with anti-muscarinic properties. Notably, clemastine treatment has been shown to promote oligodendrocyte precursor cell (OPC) differentiation *in-vitro* (Mei et al., 2014), enhance remyelination in mouse models of demyelination (Mei et al., 2014; Chan et al., 2004; Li et al., 2015; Deshmukh et al., 2013), and has shown promise as a treatment for patients with multiple sclerosis (Abdelhak et al., 2022; Cordano et al., 2022). Moreover, clemastine treatment rescued behavioral changes in socially isolated mice, which was attributable to increased myelination within the prefrontal cortex (Liu et al., 2016), and was found to reverse cognitive dysfunction in the APP/PS1 mouse model of Alzheimer’s disease in a manner that was associated with improved memory-related task performance (Chen et al., 2021a). Finally, clemastine treatment increased remyelination following cuprizone-induced demyelination and was able to rescue schizophrenia-like behavioral changes in this model (Li et al., 2015).

In the current set of experiments we sought to determine if prophylactic, daily, oral clemastine treatment, could rescue behavioral and neurocognitive deficits brought on by IAV in adult mice. We found that treatment caused a slight improvement in weight loss associated with infection, which was most prominent in male mice. Additionally, treatment was sufficient to reverse neurocognitive deficits caused by IAV infection, as assessed by the Morris water maze (MWM) test, but did not affect changes to burrowing behavior. Importantly, mice treated with clemastine neither displayed increased lung viral RNA, nor altered *Ifng* expression at a time-point corresponding to peak sickness. Instead, clemastine treated mice exhibited increased virus-specific humoral responses, indicating clemastine did not adversely affect the generation of adaptive immunity to IAV. Peripheral IAV infection increased hippocampal mRNA levels of *Tnf* and *Cdkn1a*, and concurrently decreased expression of *Plp1* and *Ugt8a*. Clemastine treatment neither affected infection-induced changes in *Tnf* nor *Cdkn1a* levels and did not significantly reverse changes to *Plp1*, *Ugt8a* or *Mag* expression.

2. Materials and methods

2.1. Mice, clemastine treatment and infection

All animal care protocols were in accordance with National Institutes of Health Guidelines for Care and Use of Laboratory Animals and were approved by the University of Illinois Institutional Animal Care and Use Committee (protocol number 22083). Six-week-old male and female C57BL/6J mice were obtained from Jackson Laboratories (No. 000664). Upon arrival, animals were tail-marked and randomized into one of four groups by sex, based on treatment and infection: Vehicle/Saline, Clemastine/Saline, Vehicle/IAV and Clemastine/IAV. In total, three cohorts of mice were used to assess the effect of infection and treatment on learning and memory (Fig. 1a) and two cohorts of mice were used to assess the effects of infection and treatment on burrowing activity and immune cell responsiveness and viral RNA in the lung (Fig. 1b). Morris water maze testing, for each cohort of mice, was performed continuously between the hours of 10:00am and 7:00pm. Burrowing behavioral tests were initiated at 10:00am and food burrowed measured 24h later. At the end of each experiment euthanasia was initiated at 1:00pm.Mice were housed four per cage under constant 12-h light/dark cycles (10am-10pm), average daily temperature 22.51 ± 0.143 (S.E.M.; range, 20.56–23.89 °C) and average daily humidity55.7 ± 1.97 (S.E.M.; range, 37–65%) and allowed to acclimate for one week prior to the commencement of prophylactic treatment.

Clemastine treatment at a dose of 10 mg/kg/d by oral gavage has been shown to promote myelination and remyelination (Mei et al., 2014), rescue behavioral changes caused by social isolation (Liu et al., 2016), mitigate chemotherapy-induced cognitive impairment (Chen et al., 2022), improve cognitive dysfunction in a the APP/PS1 Alzheimer’s Disease model (Chen et al., 2021b), and restore behavioral changes caused by cuprizone intoxication (Li et al., 2015) as well as reverse myelination deficits resulting from prenatal hypoxia (Cree et al., 2018). Based on these results, mice were treated with clemastine at a dose of 10 mg/kg/d. Clemastine (Selleckchem, S1847) was initially dissolved in dimethyl sulfoxide (DMSO; Sigma, D2650) at a concentration of 10 mg/ml at 37 °C for 1 h then diluted to a working concentration in sterile water such that mice received a dose of 10 mg/kg in a 200 μl volume by oral gavage. Treatment with vehicle or clemastine (10 mg/kg/d, approximately 9:00am each day) was commenced one week after mouse arrival and one week prior to virus inoculation. Mice were treated daily for the duration of the experiment (Fig. 1).

At eight weeks of age, mice were anesthetized with 3% isoflurane and then intranasally inoculated with either sterile phosphate buffered saline (PBS), or PBS containing 100 plaque forming units (PFU) of mouse-adapted human influenza A virus strain A/Puerto Rico/8/1934 (H1N1) (A/PR8) from American Type Culture Collection (ATCC, VR-95)

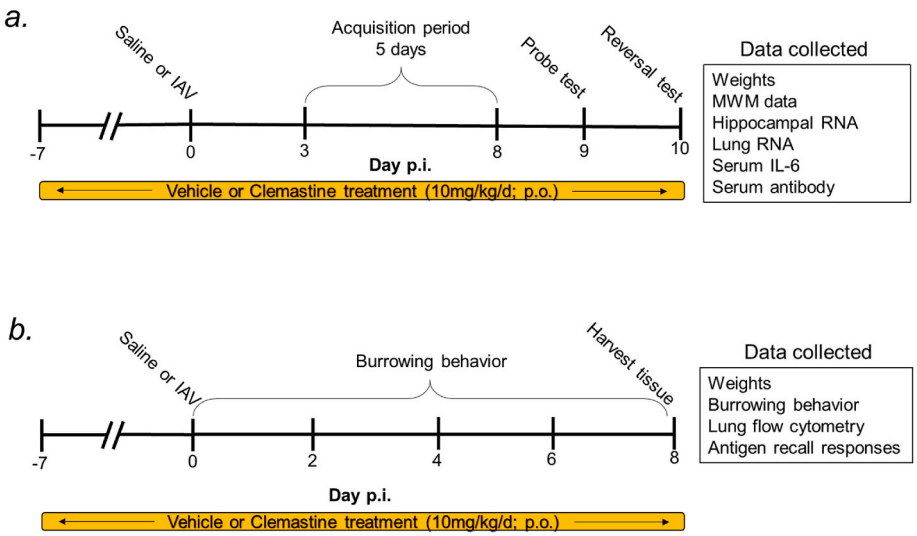

Fig. 1. Experimental design for Morris water maze testing and burrowing behavior cohorts. Male and female C57BL/6 mice were treated with vehicle or clemastine (10 mg/kg/d) by oral gavage for one week prior to being inoculated intranasally with saline or IAV (100 p.f.u.). Treatment continued throughout the course of infection. **a,** The experimental design used to assess the effects of infection and treatment on learning, memory and cognitive flexibility. For these tests, three replicative cohorts containing a total of N = 17–20 mice per group were used. **b,** The experimental design for burrowing behavioral testing comprising two replicative cohorts, containing a total of N = 10–11 mice per group were used.

in a total volume of 0.03 ml, as described previously (Louie et al., 2023). For each experiment mice were inoculated with saline or IAV at 10:00am, after receiving their daily treatment of vehicle or clemastine. Animal weights were measured daily prior to behavioral measurements. Percent weight change was calculated from day 0 post-infection (p.i.).

Mice were euthanized by CO_2 asphyxiation at time points corresponding to the completion of Morris water maze (MWM) testing (day 10 p.i.) or peak sickness, as determined previously by changes to weight, burrowing behavior and adaptive immune responses (day 8 p.i.) (Louie et al., 2022, Louie et al., 2023).

2.2. Morris water maze

The effects of treatment on infection-induced alterations in spatial learning and memory was assessed using by MWM, which is a hippocampal-dependent task (Schenk and Morris, 1985; D'Hooge and De Deyn, 2001) (Fig. 1a). The MWM and consisted of a circular pool (122 cm diameter, Noldus) with a transparent round platform (10 cm diameter; Noldus) hidden 1 cm below the surface of the water. Water temperature for all tests was kept between 23 and 25 °C. To determine if treatment or infection altered the capacity to learn, acquisition testing was initiated at day 3 p.i., which corresponds to initial reductions in body weight due to infection (Louie et al., 2022), and was performed for five consecutive days corresponding to day 3-7 p.i. During the acquisition phase, the platform position remained constant and the mice were trained to use distal visuospatial cues to navigate a path to the hidden platform. At the start of each testing session, mice were placed on the platform for 15 s. For each acquisition testing day, mice were subjected to three trials, which were conducted using a pseudorandom protocol, with mice placed in the water from one of three entry locations. During the test, the mice were allowed to freely swim for 60 s or until they reached the platform. If the platform was not located within 60 s, the mice were guided to the platform and allowed to remain on it for 15 s. After three consecutive trials, the mice were placed in their home cage to dry. Memory was assessed by probe trial on day 8 p.i. Specifically, 24 h after the last day of acquisition testing mice underwent a probe trial wherein the hidden platform was removed, and the mice were allowed to swim for 60 s in order to assess spatial memory for the platform location. Finally, the effect of infection and treatment on cognitive flexibility was assessed by reversal trial on day 9 p.i. For this test, the hidden platform was moved to the opposite quadrant of the pool while keeping the distal visual cues constant. Mice were placed on the platform for 15 s, then they were given three trials to locate the platform in the new target quadrant. The reversal test measured how quickly the mice were able to extinguish their initial learning and acquire the new location (Vorhees and Williams, 2006). Velocity, latency to the platform, and distance swam (pathlength to the platform) were recorded and analyzed using a video camera and Ethovision version 14.0.1318 (Noldus Information Technologies, Netherlands). For practical reasons mice were euthanized on day 10 p.i., at which time serum and hippocampus were collected for analysis.

2.3. Burrowing behavior test

Sickness behavior was assessed using the burrowing behavior test as described previously (Louie et al., 2022) (Fig. 1b). In brief, mice were presented with a slanted polyvinyl chloride tube containing a pre-measured amount (~200 g) of food pellets on days 0, 2, 4, 6, and 8 p.i. The contents of the tube were measured after 24h and percentage of burrowed food determined. We have found that this measurement is a sensitive measure of sickness behavior during IAV infection and that there are maximal reductions in burrowing behavior at day 8 p.i. (Louie et al., 2022).

2.4. RNA extraction and data analysis

At day 8 p.i. lungs were collected, immediately flash frozen in liquid nitrogen, and stored at −80 °C until they could be further processed. At day 10 p.i. brains were bisected longitudinally and preserved in RNA later. Frozen lungs were pulverized into a homogenized powder using a mortar and pestle (Cole-Parmer) on dry ice and RNA was extracted by TRIzol (ThermoFisher, 15596026) then column-purified using the GeneJET RNA purification kit (ThermoFisher, K0732) as per the manufacturer's instructions. Purified RNA quantity was determined by a NanoDrop ND-1000 spectrophotometer (ThermoFisher) and quality determined by running samples on a 1% agarose gel. The hippocampus of each mouse brain was dissected, and homogenized for RNA extraction with TRIzol and processed as described for the lungs. Following isolation, RNA was converted into cDNA using the Reverse Transcription System (Promega, A3500) according to manufacturer's instructions in a

C1000 Touch Thermal Cycler (Bio-Rad Laboratories). Gene expression levels of viral *M1*, as well as the inflammatory cytokines *Ifng* and *Tnf* from lung tissue was determined by quantitative RT-qPCR using *PowerSYBR®* green according to the manufacturer's instructions (ThermoFisher, 4367659) and were normalized to *Gapdh*. All primers for lung gene expression were from (Integrated DNA Technologies). TaqMan Gene Expression Probe Assays (Integrated DNA Technologies) were used to determine brain gene expression of inflammatory markers *Tnf* and *Cdkn1a*, as well as oligodendrocyte specific genes *Ugt8a, Plp1*, and *Mag* according to the manufactuer's instructions. Expression values of brain genes were normalized to *Actb*. Subtle differences in gene expression procedures were due to the amplification of viral *M1* by PowerSYBR® green as described previously (Blackmore et al., 2017). Thus, all lung gene expression was determined using the same technique. Primer and probe sequences can be found in Table 1. Regardless of tissue origin, expression levels were calculated using the $2^{-\Delta\Delta Ct}$ method.

2.5. Flow cytometry

Flow cytometry was used to assess the effect of treatment on lung infiltrating immune cells as described previously (Louie et al., 2022). Briefly, at day 8 p.i. single-cell suspensions were prepared from lungs by enzymatic digestion then 1×10^6 cells were incubated with anti-CD16/32 (14-0161-82; clone 93, ThermoFisher) for 10 min to block Fc receptors. Cells were then stained with antibodies against the following surface markers for 20 min while on ice: Ly-6G eFluor™ 450 (ThermoFisher, 48-9668-82), Ly-6C PE-Cyanine7 (ThermoFisher, 25-5932-32), CD45 APC (ThermoFisher, 17-0451-83), CD19 PE-eFluor 610 (ThermoFisher, 61-0193-82), CD8a Super Bright 645 (ThermoFisher, 64-0081-82), CD3e Alexa Fluor® 488 (ThermoFisher, 53-0081-82), CD11 b PE (BioLegend, 101208), eBioscience™ Fixable Viability Dye eFluor™ 780 (ThermoFisher, 65-0865-14). After washing, samples were run on an Attune NxT flow cytometer (ThermoFisher), and data were analyzed using FlowJo software (v10.7.2). Gates were determined using unstained and fluorescence minus one (FMO) samples. Compensation for all channels except viability dye was determined using single-stained compensation beads (01-2222-42; ThermoFisher). Viable, single cells were then gated using the immune cell marker CD45. Cytotoxic T cells (Tc) were defined as $CD45^+CD3^+CD8^+$ and helper T cells (Th) defined as $CD45^+CD3^+CD8^-$. B cells were identified as $CD45^+CD19^+CD11b^-$. Monocytes and neutrophils were identified as $CD45^+CD11b^+Ly6C^{hi}$ and $CD45^+CD11b^+Ly6C^{int}Ly6G^+$, respectively.

2.6. Effect of treatment on virus-specific antigen recall response

The effect of infection and clemastine treatment on IAV-specific T cell response was determined by antigen recall assay as described previously (Louie et al., 2022). In brief, single-cell suspensions from spleens were generated from male and female mice at day 8 p.i. and plated at a density of 5×10^5 cells per well in a round-bottom 96-well plates in 200 µl RPMI 1640 supplemented with 10% FBS, L-glutamine, and 1% penicillin/streptomycin. After plating, the splenocytes were cultured with media alone, an irrelevant viral peptide derived from Theiler's murine encephalomyelitis virus ($VP2_{121–130}$), or one of two immunodominant MHC class I–restricted peptides of A/PR8 IAV ($NP_{366–374}$, $PA_{224–233}$) at a concentration of 2 µM. Peptides were from Anaspec (Fremont, CA). All samples were run in triplicate. Following stimulation for 72 h, the plate was frozen at −80 °C. IFN-γ levels were determined by ELISA (ThermoFisher, 88-7314-88) according to the manufacturer's instructions. The assay range for IFN-γ is 16–2000 pg/ml.

2.7. Effect of treatment on serum virus-specific antibody and IL-6 levels

After asphyxiation with CO_2, blood was isolated from the heart and collected into 1.5 ml polypropylene tubes then allowed to clot at 4 °C. The blood was centrifuged at 2000×*g* for 10 min and the serum was removed and stored at −80 °C until use. To measure virus-specific antibody responses recombinant hemagglutinin (HA) protein from Influenza A H1N1 virus (strain A/Puerto Rico/8/1934; ThermoFisher, A42599) was diluted to a concentration of 2.5 µg/ml in PBS. High protein-binding 96-flat bottom plates (ThermoFisher, 44-2404-21) were then coated overnight with 0.25 µg HA viral membrane protein per well in a total volume of 100 µl per well at 4 °C. Following the overnight incubation, the plates were washed five times with PBS containing 0.05% Tween 20 (Sigma, P2287) at a volume of 200 µl per well. Plates were then blocked with ELISA diluent (BioLegend, 421203), 200 µl/well, for 1h at room temperature, then washed as described previously. Mouse serum samples from day 10 p.i. were serially diluted (1:20, 1:40, 1:80, 1:160) in ELISA diluent, 100 µl added to each well and samples were incubated for 1.5 h at room temperature. After aspirating and washing five times, the plates were incubated with either goat anti-mouse peroxidase conjugated IgM antibody (Sigma, A8786) or goat anti-mouse peroxidase conjugated IgG antibody (Sigma, A5278) diluted 1:10,000 in ELISA diluent for 1 h at room temperature. After washing seven times, 100 µl of 3,3′,5,5′-Tetramethylbenzidine (TMB) substrate solution (ThermoFisher, N301) was added to each well for 5 min, then the reaction was stopped by adding 50 µl of 2N sulfuric acid. Data are

Table 1
Primers and probes used for gene quantitation.

Tissue	Gene	Primer sequence	Probe seqeunce
Brain	*Actb*	F: 5′-GATT ACTGCTCTGGCTCCTAG-3′ R: 5′-GACTCATCGTACTCCTGCTTG-3′	5'-/56-FAM/CTGGCCTCA/ZEN/CTGTCCACCTTCC/31ABkFQ/-3′
	Cdkn1a	F:5′-GAAGAGACAACGGCACACT-3′ R:5′-CAGATCCACAGCGATATCCAG-3′	5'-/56-FAM/TTCAGAGCC/ZEN/ACAGGCACCATGT/3IABkFQ/-3′
	Mag	F: 5′-AGAGAGCAGAGATGGACAGT-3′ R: 5′-CACCATACAACTGACCTCCAC-3′	5'-/56-FAM/CATCGTCAA/ZEN/CACCCCCAACATTGTG/31ABkFQ/-3′
	Plp1	F: 5′-GTTCCAAATGACCTTCCACCT-3′ R: 5′-ATGAGTTTAAGGACGGCGAAG-3′	5'-/56-FAM/CACACTAGT/ZEN/TTCCCTGCTCACCTTCA/31ABkFQ/-3′
	Tnf	F:5′-AGACCCTCACACTCAGATCA-3′ R:5′-TCTTTGAGATCCATGCCGTTG = −3′	5'-/56-FAM/CCACGTCGT/ZEN/AGCAAACCACCAAGT/31ABkFQ/-3′
	Ugt8a	F: 5′-CAAGACCAACGCTGCCT AA-3′ R: 5′-CATGTTCCTGAGCACCACTT-3′	5'-/56-FAM/AGCCCACTG/ZEN/CCAGAAGATCTGC/31ABkFQ/-3′
Lung	*M1*	F: 5′-AAGACCAATCCTGTCACCTCTGA-3′ R: 5′-CAAAGCGTCTAC GCTGCAGTCC-3′	No probe
	Ifng	F: 5′-ACTGGCAAAAGGATGGTGAC-3′ R: 5′-TGAGCTCATTGAATGCTTGG-3′	No probe
	Tnf	F: 5′-TGTCCCTTTCACTCACTGGC-3′ R:5′-CATCTTTTGGGGGAGTGCCT-3′	No probe
	Gapdh	F5′-GCATCTTCTTGTGCAGTGCC-3′ R:5′-TACGGCCAAATCCGTTCACA-3′	No probe

presented as optical density at 450 nm.

Serum IL-6 levels were determined by ELISA according to the manufacturer's instructions (ThermoFisher, 88-7064-88). The assay range for IL-6 is 4–500 pg/ml.

2.8. Statistical analyses

GraphPad Prism software (ver. 9.1.0) was used for statistical analyses. Weight change, burrowing, acquisition data from the MWM and virus-specific antibody levels were assessed by repeated-measures analysis of variance (ANOVA) followed by Tukey's correction for multiple comparisons. Analysis of mRNA levels, cytokine production and reversal trial analyses for the MWM were performed using three-way ANOVA followed by Tukey correction for multiple comparisons. Outliers were checked by ROUT test where Q = 1%. In the few cases where outliers were detected their removal did not influence the data interpretation and thus all data were included in the analysis and are represented in the figures. Correlations between burrowing behavior and weight change amongst infected mouse groups was assessed by Pearson correlation. Results are presented as means ± S.E.M. where individual points represent a single mouse.

3. Results

3.1. Clemastine treatment partially reversed virus-induced changes to body weight

Change in percent body weight was used as a proxy for assessing sickness and morbidity following infection (Fig. 1a–b). Regardless of sex, mice inoculated with IAV displayed a decrease in body weight, an effect that was partially reversed by clemastine treatment (Fig. 2a; Suppl. Fig. 1a). However, despite being inoculated with an equal infectious dose of IAV, female mice lost more weight compared to male mice and treatment had a more pronounced effect on weight loss in male mice compared to female mice (Suppl. Fig. 1a). The weight loss data are consistent with the findings from others that indicate female mice exhibit increased morbiditiy following experimental infection with the PR8 strain of IAV(52,53).

3.2. Clemastine treatment alterations to cognitive flexibility caused by IAV infection

The MWM test is commonly used to assess spatial learning (acquisition trials), memory (probe trial) and cognitive flexibility (reversal trial). When infected with IAV, male mice exhibited a decrease in their cognitive flexibility (Jurgens et al., 2012). As clemastine treatment was previously shown to improve cognitive function in various animal

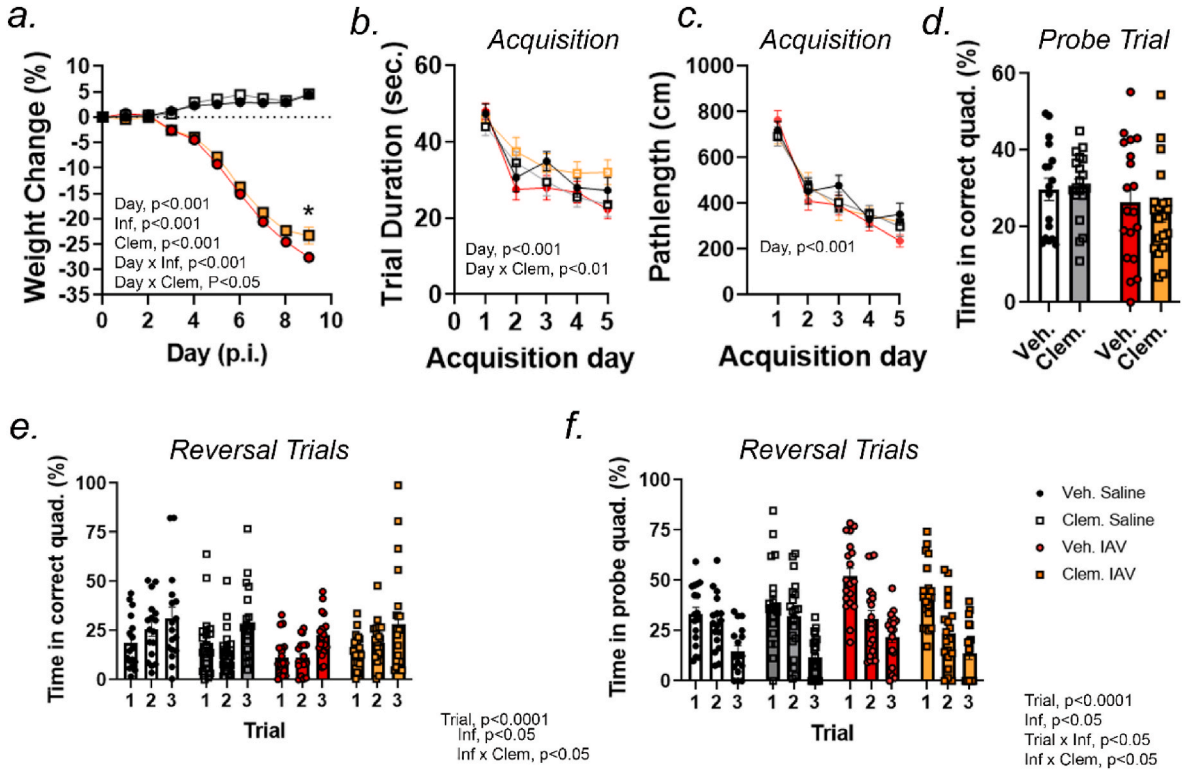

Fig. 2. Prophylactic clemastine treatment reverses IAV-induced cognitive impairment. a-d, Male and female C57BL/6 mice were treated with vehicle or clemastine (10 mg/kg/d) by oral gavage for one week prior to being inoculated intranasally with saline or IAV (100 p.f.u.). Treatment continued throughout the course of infection. The effect of infection and treatment **(a)** on changes to body weight from all cohorts of mice. Results are means ± S.E.M. from male and female mice together; n = 27–31 mice per group. Significance was determined by 3-way repeated measures ANOVA with Tukey post-hoc analysis. Main effects of day, infection and clemastine treatment are shown. Significance levels from post-hoc analysis *, $p < 0.05$. **b-c,** The effect of infection and treatment on memory acquisition trials as assessed by trial duration **(b)** and distance traveled to hidden platform **(c)** during acquisition days 1–5 (days 3-7 p.i.). Results are means ± S.E.M. from male and female mice together; n = 17–20 mice per group. Significance was determined by 3-way repeated measures ANOVA with Tukey post-hoc analysis. Main effect of day is indicated. The effect of infection and treatment on time spent in the correct quadrant during the probe trial **(d)**. Results in **d** are means ± S.E.M. from male and female mice together; n = 17–20 mice per group. Significance was determined by 2-way ANOVA. **e-f,** Effect of infection and treatment on time spent in the correct new quadrant **(e)** as well as incorrect quadrant used in acquisition and probe testing **(f)**. Data are means ± S.E.M. from males and females and are from n = 17–20 per group. Significance was determined by 3-way ANOVA with Tukey post-hoc analysis. Main effects of trial, infection (Inf) as well as trial x infection (Trial x Inf) and infection x treatment (Inf x Clem) interaction are shown.

models of disease (Pan et al., 2020; Chen et al., 2021b; Cree et al., 2018; Barak et al., 2019), we questioned whether treatment would reverse the cognitive impairment brought on by infection. Therefore, male and female mice were randomized into treatment groups and the effect of prophylactic clemastine treatment on cognition was assessed by MWM (Fig. 1a).

During the acquisition training phase, mice inoculated with IAV developed a pronounced reduction in swimming velocity, which was not significantly affected by treatment (Suppl. Fig. 1b). Nevertheless, there was a time-dependent reduction in both the trial duration and the distance traveled that was required to find the hidden platform, indicating an ability to learn, which was not affected by either infection or clemastine treatment (Fig. 2b–c). Given the effect of sex on changes to weight, we next questioned whether swimming velocity, trial duration or swimming distance to the hidden platform was differentially affected in IAV-inoculated male and female mice. Virus-induced changes in swimming velocity did not differ between male and female mice (Suppl. Fig. 1c). However, infected female mice took longer to find the hidden platform than infected male mice during the aquistion trial (Suppl. Fig. 1d), although there was no significant effect of sex on distance traveled (Suppl. Fig. 1e). Interestingly, the increased trial duration amonst infected female mice was attributable to clemastine treatment (Suppl. Fig. 1d). Nevertheless, these data are in line with those previously published (Jurgens et al., 2012), which indicate that infected mice develop decreased swimming velocity, but display a similar capacity to learn when compared to saline-inoculated mice.

To determine whether infection or treatment affected spatial memory, a probe trial was conducted on day 8 p.i. (Fig. 1a). For this test, the hidden platform was removed and the percentage of time spent in the correct quadrant determined. There was neither an effect of infection nor treatment on performance in the probe trial (Fig. 2d). However, considering sex as a variable revealed that female mice spent less time in the correct quadrant compared with male mice, an effect likely attributable to differences between infected females and all other groups (Suppl. Fig. 1f). In contrast, the performance of infected male mice did not differ from non-infected male mice in the probe trial, as observed previously (Jurgens et al., 2012). Again, these data are consistent with the observation that female mice exhibited increased morbidity as a result of infection.

Finally, cognitive flexibility was assessed on day 9 p.i. using three reversal trials. For these trials the hidden platform was moved to the quadrant opposite to that of the probe trial, mice were placed on the platform in its new location for 15 s, then placed in the water at one of three starting positions. To ensure that mice had a preference for the correct quadrant containing the hidden platform, the percentage of time in the new correct quadrant as well as the previous quadrant used for the probe test was determined. Compared to saline-inoculated control mice, infected mice spent less time within the correct quadrant containing the hidden platform (Fig. 2e), but more time in the incorrect quadrant (Fig. 2f), strongly suggesting that infection reduced cognitive flexibility, as shown previously (Jurgens et al., 2012). Notably, the effect of infection on both the percentage of time spent in the correct quadrant as well as the time spent in the incorrect probe quadrant was reversed by prophylactic clemastine treatment (Fig. 2e–f).

To assess whether sex had an effect on reversal trial performance, the percentage of time that mice spent in the correct quadrant and incorrect probe quadrant was compared between male and female infected mice. Time spent in the correct quadrant during reversal testing was not different between male and female mice (Suppl. Fig. 1g), whereas female mice were found to spend less time in the incorrect probe quadrant than male mice (Suppl. Fig. 1h). Finally, the effect of trial, infection and treatment on total pathlength to the hidden platform was compared across groups. In general, the mean pathlength to the hidden plaform tended to be reduced as a result of continued trials (main effect of trial, $p < 0.05$), except in infected groups (trial by infection interaction, $p < 0.05$). However, there was no significant effect of clemastine treatment. Furthermore, comparisons between IAV-inoculated male and female indicated that pathlength between male and female mice did not differ (Suppl. Figs. 1i–k). Collectively, the data indicate that infected mice exhibit a decrease in cognitive function, as they spent more time in the incorrect quadrant that previously contained the platform and less time in the correct quadrant that contained the new location of the platform than non-infected mice and that clemastine treatment alleviated this effect to some extent.

3.3. Treatment did not affect infection-induced changes to burrowing behavior

The burrowing test measures motivation to perform an intrinsically ingrained task in rodents (Deacon, 2006). We previously found that infected male mice developed reduced burrowing activity that became evident by day 4 p.i. and persisted through day 10 p.i. (Louie et al., 2022). While burrowing behavior is not a measure of cognition, it has been used to predict pathological changes to the hippocampus (Deacon et al., 2001; Deacon and Rawlins, 2005). To determine if clemastine treatment was capable of ameliorating infection-induced changes in burrowing activity, we first analyzed the data without considering sex as a variable. As in previous studies (Louie et al., 2022), infected mice exhibited a decrease in their burrowing response compared to saline-inoculated controls beginning at day 4 p.i. and being maximal at day 8 p.i. (Fig. 3a). These time points post infection correspond precisely to when mice decrease their food intake (Louie et al., 2022), and in the current study, changes in burrowing response was found to correlate with changes in weight (Fig. 3b), indicating that alterations to burrowing behavior by IAV may also be linked to changes in motivation or indicative of lethargy. Having established an effect of infection, we next examined the effects of sex and treatment on changes in the burrowing response caused by infection with IAV. While there was no effect of sex on burrowing behavior, IAV-inoculated male mice treated with clemastine exhibited decreased burrowing compared to vehicle-treated controls, an effect that was not observed in female mice (Suppl. Fig. 2). These data show that the effects of infection on burrowing response was not improved by clemastine treatment, at least at the time points examined.

3.4. Treatment did not adversely affect the generation of anti-viral immune responses

Muscarinic receptors are expressed by lymphocytes and have been shown to influence immune function (Halder and Lal, 2021; Cameron et al., 1986). Alterations in immune responsiveness and/or viral load by treatment may have contributed to changes in cognitive capacity. As such, we sought to determine the effects of clemastine treatment on the generation of virus-specific immune responses and lung viral load. We first examined whether treatment altered lung-infiltrating immune cell populations, including T cells, B cells and myeloid cells (Fig. 4a), by flow cytometry at day 8 p.i., a time point which we previously found corresponds to robust infiltration of adaptive immune cells (Louie et al., 2022). We observed no change in the percentage of $CD3^{+}CD8^{-}$ helper T (Th) cells across groups (Fig. 4b). However, infection increased the percentage of $CD3^{+}CD8^{+}$ cytotoxic T (Tc) cells and decreased the percentage of $CD19^{+}$ B cells (Fig. 4d). Infection also increased $CD11b^{+}Ly6C^{hi}$ monocytes, and $CD11b^{+}Ly6G^{+}$ neutrophils within the lung (Fig. 4e–f). Clemastine treatment did not alter the percentage of any immune cell population examined (Fig. 4b–f). Infected female mice had an increased percentage of neutrophils within the lungs compared to infected male mice (Suppl. Fig. 3a). These data are in line with our previous findings that the percentage of weight loss was highly correlated with the number of lung infiltrating granulocytes (Louie et al., 2022).

It is possible that clemastine reduced the generation of virus-specific immune responses without affecting the percentage of infiltrating

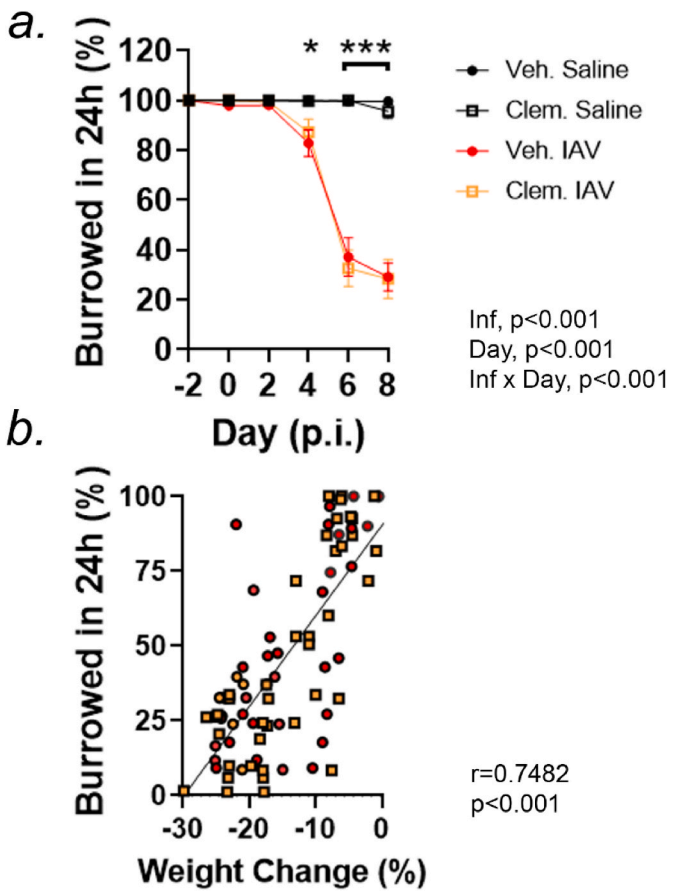

Fig. 3. Burrowing behavior was not affected by clemastine treatment but was correlated with weight change. a-b, Male and female C57BL/6 mice were treated with vehicle or clemastine (10 mg/kg/d) by oral gavage for one week prior to being inoculated intranasally with saline or IAV (100 p.f.u.). Treatment continued throughout the course of infection. **a,** Burrowing behavior was assessed every other day until day 8 p.i. Results are from male and female mice together; n = 10–11 mice per sex per group. Significance was determined by 3-way repeated measures ANOVA with Tukey post-hoc analysis. Main effects of infection (Inf), day as well as the interaction between infection and day (Inf x Day) are shown. **b,** Data from infected mice were beginning at day 2 p.i. were used to assess correlations between burrowing behavior and changes to weight by Pearson correlation.

immune cells in the lung. Therefore, to determine if treatment affected the generation of virus-specific cytotoxic T cells we performed antigen recall assays on primary splenocytes isolated at day 10 p.i., in which cultures were stimulated with immunodominant H-2D^b–restricted peptides from either IAV ($PA_{224–233}$, $NP_{366–374}$) or a non-specific virus (TMEV; $VP2_{121–130}$) and IFN-γ production was assessed by ELISA. Splenocytes from IAV-inoculated mice readily produced IFN-γ following stimulation with both IAV-specific peptides (Fig. 5a–b), whereas little to no IFN-γ was produced in response to the control peptide (Fig. 5c). Clemastine treatment did not affect IFN-γ production in response to IAV-specific peptide stimulation. However, a comparison between infected male and female mice indicated that splenocytes from female mice produced more IFN-γ in response to IAV-specific peptide stimulation than those from male mice (Suppl. Fig. 3b).

To assess whether treatment altered the generation of an adaptive humoral response, we measured levels of virus-specific (HA-reactive) IgM and IgG levels in serum at day 10 p.i. Both antibody isotypes were substantially elevated in serum isolated from infected mice. Moreover, circulating levels of virus-specific IgM were increased by clemastine treatment (Fig. 5d), while virus-specific IgG levels were unaffected (Fig. 5e). Having established an effect of infection, we next excluded saline-inoculated controls in order to examine the effects of sex and treatment on the generation of virus-specific antibody levels. This analysis revealed that males had slightly increased levels of both virus-specific IgM and IgG compared to females. While clemastine treatment increased levels of serum anti-viral IgM in both sexes, treatment only increased levels of anti-viral IgG in male mice and did not affect levels in female mice (Suppl. Figs. 3c–d).

The above indicated that treatment did not cause immunosuppression and likely did not adversely affect viral load within the lungs. To test whether this was the case, we measured expression of viral *M1*, *Ifng* and *Tnf* transcripts in the lungs by RT-qPCR at day 10 p.i. Both viral *M1* and *Ifng* expression were readily detectable in the lungs of infected mice. Whereas, there was no significant effect of infection on expression levels of *Tnf* at this time point. Clemastine treatment did not affect the expression of either *M1*, *Ifng* or *Tnf* (Fig. 5f–h), indicating that treatment neither caused immunosuppression nor affected viral RNA levels within the lung.

It is notable that clemastine treatment has been shown to suppress circulating levels of IL-6 in response to experimental bacterial infection (Johansen et al., 2011). Since serum IL-6 is elevated during infection (Blackmore et al., 2017), and because increased circulating IL-6 has been correlated with altered cognition, we questioned whether treatment affected serum IL-6. Mice inoculated with IAV had increased serum IL-6 at day 10 p.i., and while treatment appeared to suppress levels at this time point, the effect did not reach statistical significance ($p = 0.063$). Finally, there was no effect of sex on circulating IL-6 levels (Suppl. Fig. 4).

3.5. Infection increased hippocampal expression of genes associated with neuroinflammation and concurrently decreased OL-specific genes

We previously found that IAV infected mice exhibited increased hippocampal levels of genes indicative of glial activation, such as *Tnf* and *Cdkn1a,* and that increased expression of these genes corresponded to decreased levels of OL-specific genes including *Ugt8a, Plp1* and *Mag* (Louie et al., 2023). Therefore, we sought to determine if clemastine treatment might act to influence the expression of these genes of interest. Infection increased hippocampal expression levels of both *Tnf* and *Cdkn1a*, but treatment did not affect expression of either *Tnf* or *Cdkn1a*, indicating that treatment did not improve cognitive function by inhibiting *Tnf* or *Cdkn1a* within the hippocampus (Fig. 6a–b). Also, as observed previously (Louie et al., 2023), infection decreased expression levels of the oligodendrocyte specific genes *Plp1* and *Ugt8a* in the hippocampus (Fig. 6c–d). The expression of both *Plp1* and *Ugt8a* was lower in female mice compared to male mice, and clemastine treatment did not alter expression of either of these genes. Furthermore, we observed no significant differences in hippocampal *Mag* expression between groups. However, there was trend for infection to decrease hippocampal *Mag* expression and for clemastine treatment to reverse this effect (infection by treatment interaction, $p = 0.07$; Fig. 6e). When sex was considered as a variable, infected female mice were found to have increased expression of *Tnf* and *Cdkn1a* (Suppl. Figs. 5a–b) and decreased expression of *Plp1* and *Ugt8a* when compared to male mice (Suppl. Figs. 5c–d). There were no differences in *Mag* expression between male and female mice, regardless of condition. Increased expression of *Tnf* and *Cdkn1a* coupled with a concurrent decrease in *Plp1* and *Ugt8a* in female mice compared to male mice is consistent with the finding that female mice displayed increased morbidity after infection. The inability for clemastine treatment to restore *Plp1* and *Ugt8a* expression indicate that alterations in expression of these specific genes in the hippocampus by infection is not likely to not account for changes to cognitive flexibility.

4. Discussion

In the current study, we investigated whether treatment with clemastine fumarate, could alleviate cognitive impairment brought on by

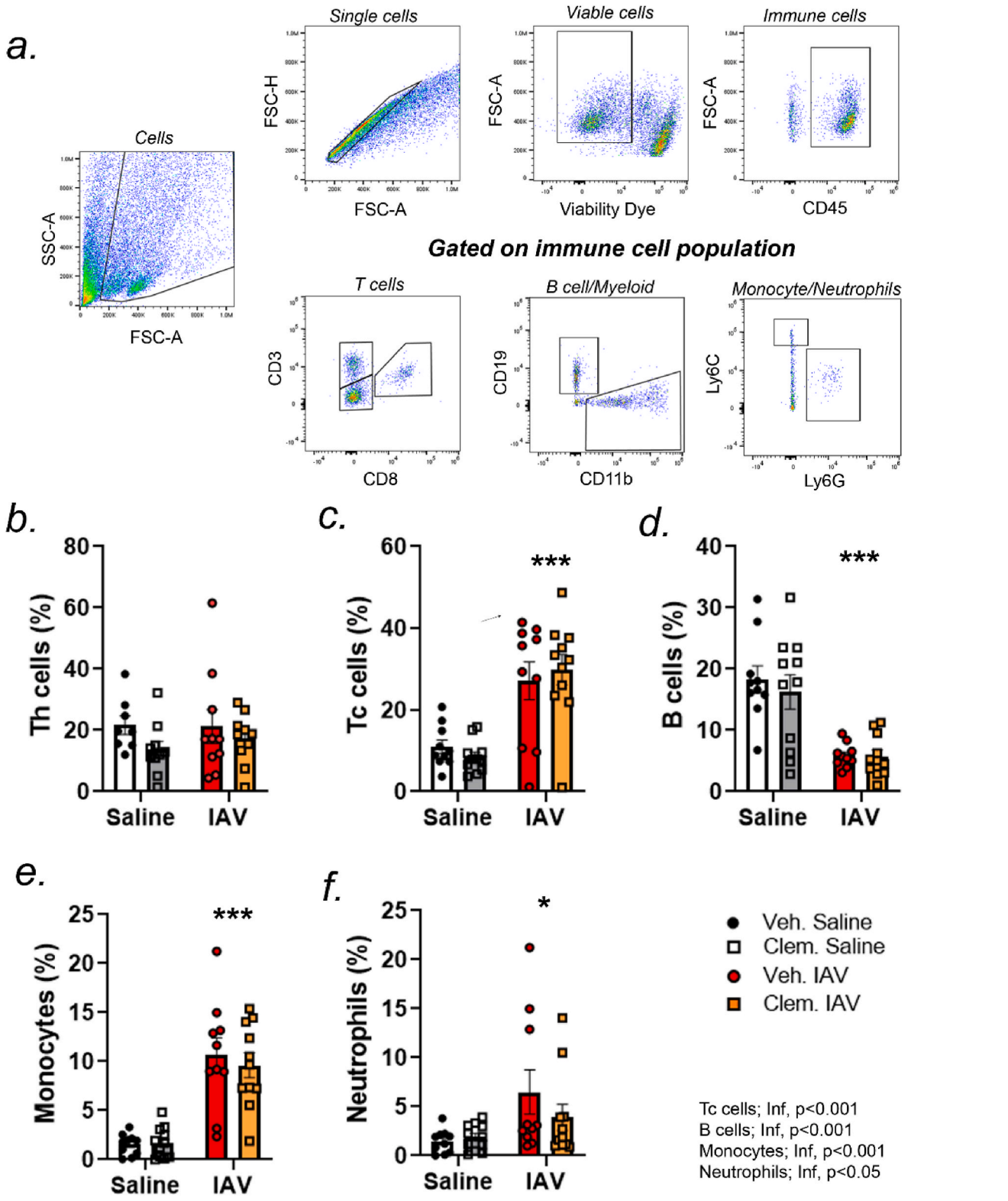

Fig. 4. Clemastine treatment alter lung immune cell infiltration. a-j, Male and female C57BL/6 mice were treated with vehicle or clemastine (10 mg/kg/d) by oral gavage for one week prior to being inoculated intranasally with saline or IAV (100 p.f.u.). Treatment continued throughout the course of infection. **a-e,** Flow cytometry was used to determine the effect of infection and treatment on lung infiltrated immune cell populations at day 8 p.i. **a,** Gating strategy for identifying adaptive and innate immune cell percentage. The effect of infection and treatment on percentages of helper T cells ($CD45^+CD3^+CD8^-$) **(b)**; cytotoxic T cells ($CD45^+CD3^+CD8^+$) **(c)**; B cells ($CD45^+CD19^+CD11b^-$) **(d)**; monocytes ($CD45^+CD11b^+Ly6C^+Ly6G^-$) **(e)**; and neutrophils ($CD45^+CD11b^+Ly6C^+Ly6G^+$) **(f)**, at day 8 p.i. Results are means ± S.E.M. from male and female mice together; n = 10–11 mice per group. Significance was determined by 2-way ANOVA with Tukey post-hoc analysis. Main effect of infection is indicated.

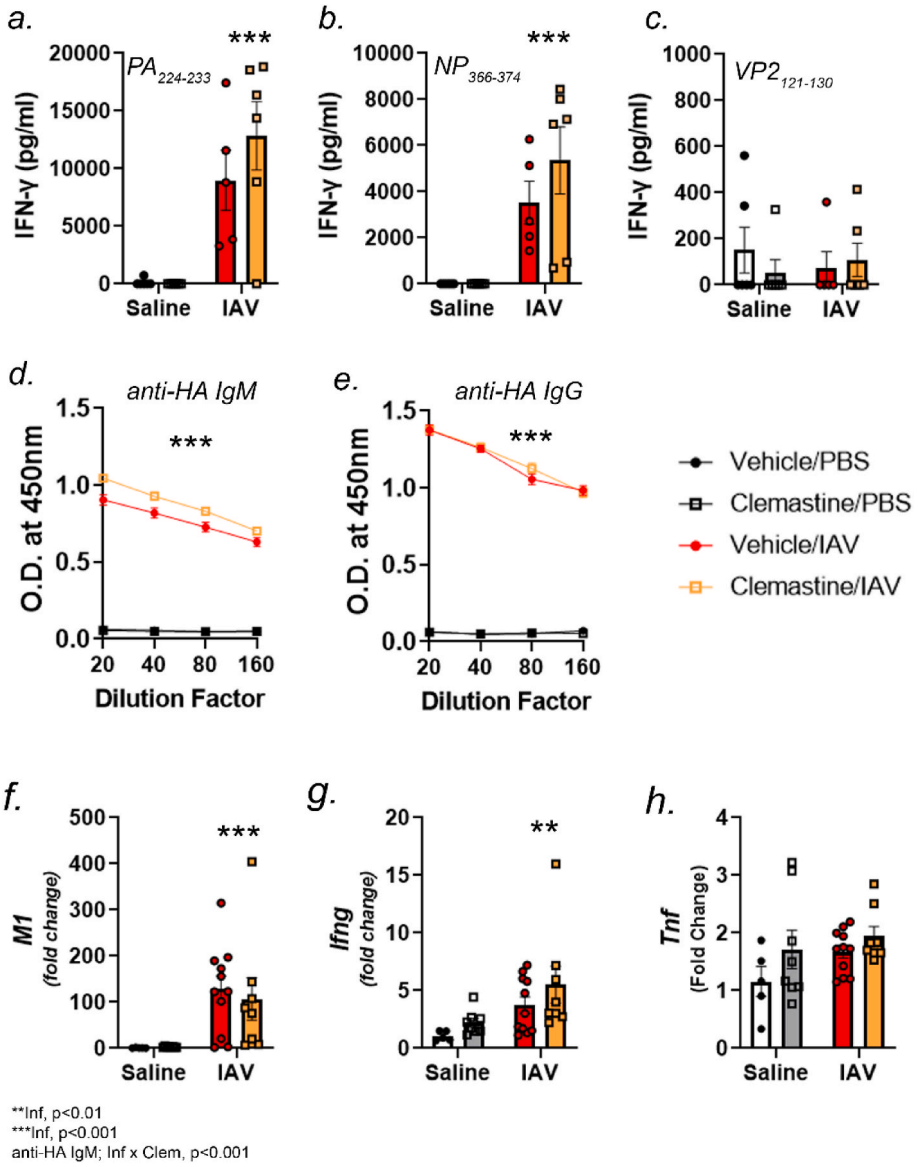

Fig. 5. Clemastine treatment did neither impaired the generation of virus-specific adaptive immune respnses. a-h, Male and female C57BL/6 mice were treated with vehicle or clemastine (10 mg/kg/d) by oral gavage for one week prior to being inoculated intranasally with saline or IAV (100 p.f.u.). Treatment continued throughout the course of infection. **a-c,** At day 10 p.i. splenocytes isolated from a subset of mice and stimulated with immunodominant MHC class I restricted peptide sequences specific to IAV (H1N1 PR8; $PA_{224-233}$ and $NP3_{66-374}$) or Theiler's murine encephalomyelitis virus ($VP2_{121-130}$) for 72h then IFN-γ levels determined by ELISA. Effect of infection and treatment on the production of IFN-γ from splenocyte cultures stimulated with $PA_{224-233}$ **(a)**, $NP3_{66-374}$ **(b)** and $VP2_{121-130}$ **(c)**. Results are means ± S.E.M. from male and female mice together; n = 5–6 per group. Significance was determined by 2-way ANOVA with Tukey post-hoc analysis. Main effect of infection is indicated. **d-e,** Effect of infection and clemastine treatment on serum IgM **(d)** and IgG **(e)** levels to recombinant H1N1 PR8 hemagglutinin (HA) as determined by ELISA at day 10 p.i. Significance was determined by 3-way repeated measures ANOVA with Tukey post-hoc analysis. Results are means ± S.E.M. from male and female mice together; n = 7–14 mice per group. **f-h,** Lung mRNA expression levels of viral *M1* (f), *Ifng* (g) and *Tnf* (h) were determined by RT-qPCR. Data are means ± S.E.M. from n = 5–11 mice per group. Significance was determined by 2-way ANOVA with Tukey post-hoc analysis. Main effect of infection (Inf) and infection x treatment (Inf x Clem) interactions are indicated.

non-neurotropic IAV infection. The results herein suggest that prophylactic treatment reversed changes to cognitive flexibility caused by infection, but that treatment did not alleviate virus-induced changes to burrowing behavior. Furthermore, we show that treatment did not adversely affect the generation of virus-specific adaptive immunity or influence levels of lung viral RNA or expression of the anti-viral cytokine *Ifng*. Rather, treatment increased virus-specific antibody levels and showed a tendency towards decreasing circulating IL-6. As in previous studies, we found that infection upregulated inflammatory markers within the hippocampus and concurrently decreased expression of the oligodendrocyte specific genes *Plp1* and *Ugt8a*. Treatment did not alter markers of inflammation, but tended to restore *Mag* expression towards baseline levels. While we cannot rule out the effects of treatment on all markers of inflammation or indices of myelin/oligodendrocyte health, the data herein indicate that clemastine treatment may alleviate cognitive impairment caused by viral infection without causing overt immunosuppression. However, the mechanism of action remains to be determined.

Current research has highlighted a role for oligodendrocytes in facilitating learning and memory. Prior investigation has shown that the degree of myelination is, in part, dependent on neuronal activity, and that processes of oligodendrogenesis and myelination adaptation is triggered in specific brain regions, including the hippocampus, in response to spatial learning (Steadman et al., 2020). Moreover,

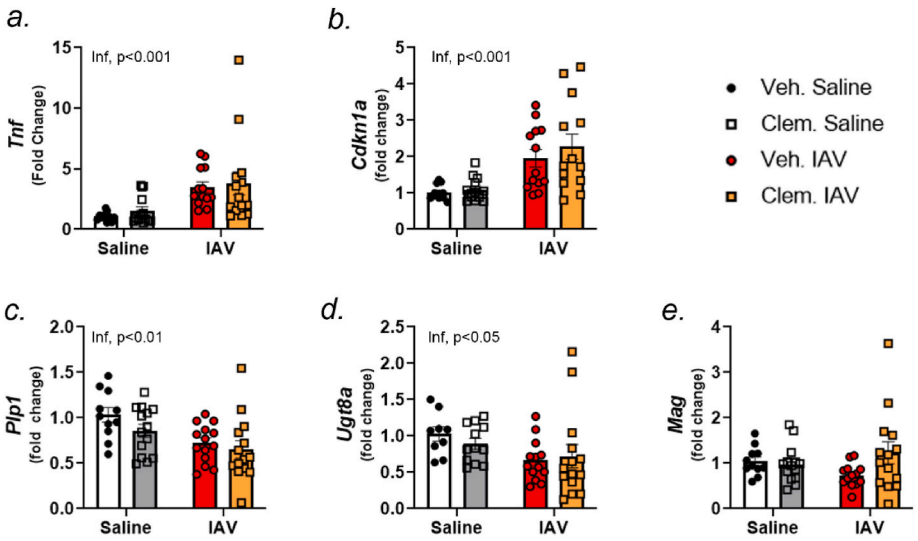

Fig. 6. Effect of treatment on markers of neuroinflammation and oligodendrocyte homeostasis in the hippocampus. a-e, Male and female C57BL/6 mice were treated with vehicle or clemastine (10 mg/kg/d) by oral gavage for one week prior to being inoculated intranasally with saline or IAV (100 p.f.u.). Treatment continued throughout the course of infection. At day 10 p.i. expression of genes associated with neuroinflammation **(a–b)** and oligodendrocyte homeostasis **(c–e)** were determined by RT-qPCR. Results are from male and female mice together; n = 5–7 mice per sex per group. Data are expressed as means ± S.E.M. Significance was determined by 2-way ANOVA with Tukey post-hoc analysis. Main effects of infection are indicated.

conditional deletion of oligodendrocyte myelin regulatory factor (*Myrf*), a transcription factor that is essential for maintaining myelin, inhibited oligodendrocyte precursor cell maturation and impaired spatial memory consolidation (Shimizu et al., 2023). Deficiency in myelination was also found to impact remote fear learning (Pan et al., 2020). Data herein show that clemastine treatment improved cognitive flexibility in IAV-infected mice, which may or may not implicate a role for oligodendrocytes in this process. While we did not measure myelination in the current study, it was recently shown that clemastine treatment improved cognitive function in an animal model of pain-induced memory impairment, and that this improvement was associated with increased hippocampal myelination (Zhu et al., 2024). The data herein show that clemastine treatment did not alter infection-induced decreases in either *Plp1* or *Ugt8a* expression. However, there was a trend towards reversing the suppressive effect of IAV on hippocampal *Mag* levels. In the CNS, MAG is located at the periaxonal space where it suspected to function in neurotropic support, myelin compaction and contribute to myelin maintenance (Quarles, 2007). Interestingly, Bacmeister et al. (2020) found that motor learning was associated with myelin remodeling, potentially implicating proteins involved in myelin membrane and/or lipid organization, such as MAG, in this process (Bacmeister et al., 2020). It is also notable that homozygous missense mutations in *MAG* have been found to underlie the development of Pelizaeus-Merzbacher-like disease, an infantile demyelinating leukodystrophy associated with motor and cognitive deficits (Lossos et al., 2015; Roda et al., 2016). Future research is needed to determine whether clemastine acts to specifically affect oligodendrogenesis, maturation, myelin remodeling or the metabolic state of oligodendrocytes during viral infection.

Clemastine is an immunomodulatory compound, but the effect of treatment on the generation of pathogen-specific immunity is limited. In previous studies, clemastine treatment was shown to suppress innate immune responses, including production of TNF and IL-6 following *Listeria monocytogenes* infection in mice, resulting in increased pathogen load and decreased survival rates (Johansen et al., 2011). The same group reported that treatment delayed the development of sepsis following an acute lipopolysaccharide challenge, which is consistent with the ability for clemastine to suppress acute phase protein production. Clemastine treatment was also shown to affect macrophage function in zebrafish following experimental infection with *Mycobacterium marinum*. However, in this model, treatment promoted inflammasome activation in a manner that was dependent on the purinergic receptor P2RX7 and limited infection (Matty et al., 2019). Interestingly, clemastine suppressed SARS-CoV-2 replication *in vitro* (Bacmeister et al., 2022). Finally, in humans, clemastine treatment reduced rhinorrhea scores during experimental (Gwaltney et al., 1996) and naturally occurring rhinoviral infection (Turner et al., 1997). As such, clemastine treatment may have alleviated virus-induced cognitive flexibility by affecting peripheral inflammation. Therefore, we assessed the effect of treatment and sex on the generation of virus-specific immunity. While the timeframe of assessment in the current study was limited to days 8 and 10 p.i., the data herein suggest that prophylactic clemastine treatment did not alter lung percentages of immune cells at a time point that corresponds to peak sickness. Instead, treatment increased IAV-specific IgM responses in both male and female mice and IgG responses in male mice. Treatment did not affect IFN-γ production in response to immunodominant MHC class I restricted IAV epitopes, and did not affect expression of lung *Ifng* or the viral *M1* gene. Finally, while the effect was not significant, there was a tendency for treatment to suppress circulating levels of IL-6 at day 10 p.i. Collectively, these data suggest that treatment did not adversely alter the generation of anti-IAV immune responses and did not cause overt immunosuppression or immune activation, but may have aided in the resolution of peripheral inflammation. As such, future studies are needed to parse out the central verses peripheral effects of clemastine treatment on virus-induced changes to cognition.

Finally, a major strength of the current study is the inclusion of both sexes in our analyses, which led to some interesting observations. As reported by others, our data demonstrate that female mice were more susceptible to IAV compared to male mice (Krementsov et al., 2017; Sabikunnahar et al., 2022; Lorenzo et al., 2011; Klein et al., 2012). Previous comparisons between male and female mice infected with IAV have consistently shown that females mount a higher anti-viral IgG response than males, especially by day 21 p.i. (Lorenzo et al., 2011; Fink et al., 2018). Virus-specific T cell responses are also reportedly higher in IAV-infected female mice compared with male mice. In line with previous findings, results from antigen recall assays to viral epitopes performed in the current study indicated that females had a higher anti-viral CD8 T cell response than males (Fink et al., 2018). In contrast to findings of others, our results show that at day 10 p.i., male

mice had higher circulating levels of anti-HA IgM and IgG compared to females. The sex effect was more pronounced for IgM than IgG. The discrepancy in anti-viral antibody responses between the current study and those of others may be attributable to the timeframes during which these responses were measured, the fact that we only assessed antibody responses to hemagglutinin rather than the whole virus, and/or antibody isotype assessed.

Sex differences in disease outcome following respiratory infections is well established and likely has multifaceted underpinnings. For instance, differential susceptibility of males and females to respiratory viral infection is partially attributable to the immunomodulatory effects of sex hormones (Cervantes et al., 2022), but also genetic variation on the Y chromosome (Krementsov et al., 2017) as well as host genotype (Sabikunnahar et al., 2022). We did not discern the specific factors contributing to sex differences in the current study. However, that male and female mice respond differently to IAV is noteworthy when attempting to interpret the effect of sex on treatment as observed by sickness behaviors as well as changes to neuroinflammatory markers since these differences were likely driven by systemic responses to infection. As such, to accurately address sex differences in neuroinflammatory responses resulting from peripheral pathogen infection, future experimental design should consider normalizing the sickness response between sexes by altering the initial pathogen load.

In conclusion, we found that IAV-induced detriments to cognitive flexibility could be improved by prophylactic treatment with the pro-myelinating drug clemastine. While the mechanisms of action remain an enigma, our data suggest that treatment did not impair the generation of anti-viral immunity. As such, the data herein suggest that clemastine may prove to be efficacious in preventing cognitive impairment and other neurological sequelae brought on by respiratory viruses such as IAV and also SARS-CoV-2.

CRediT authorship contribution statement

J.D. Tingling: Writing – review & editing, Writing – original draft, Methodology, Investigation, Formal analysis. **S.A. Krauklis:** Writing – review & editing, Investigation, Formal analysis. **P.L. Haak:** Writing – review & editing, Investigation. **R. Carr:** Investigation. **A.Y. Louie:** Writing – review & editing, Investigation. **R.W. Johnson:** Writing – review & editing, Supervision, Funding acquisition, Conceptualization. **A.J. Steelman:** Writing – review & editing, Writing – original draft, Visualization, Resources, Methodology, Funding acquisition, Formal analysis, Conceptualization.

Submission declaration and verification

The authors affirm that this manuscript has not been published previously and is not under consideration for publication elsewhere.

Declaration of generative AI in scientific writing

The authors declare that AI was not used in the writing process.

Declaration of competing interest

The authors declare no competing interests.

Acknowledgments

This research was supported by NIH 1R21NS121741 (A.J.S.).

Appendix A. Supplementary data

Supplementary data to this article can be found online at https://doi.org/10.1016/j.bbih.2024.100891.

Data availability

Data will be made available on request.

References

Abdelhak, A., Cordano, C., Boscardin, W.J., Caverzasi, E., Kuhle, J., Chan, B., Gelfand, J. M., Yiu, H.H., Oertel, F.C., Beaudry-Richard, A., Condor Montes, S., Oksenberg, J.R., Lario Lago, A., Boxer, A., Rojas-Martinez, J.C., Elahi, F.M., Chan, J.R., Green, A.J., 2022. Plasma neurofilament light chain levels suggest neuroaxonal stability following therapeutic remyelination in people with multiple sclerosis. J. Neurol. Neurosurg. Psychiatr.

Bacmeister, C.M., Barr, H.J., McClain, C.R., Thornton, M.A., Nettles, D., Welle, C.G., Hughes, E.G., 2020. Motor learning promotes remyelination via new and surviving oligodendrocytes. Nat. Neurosci. 23, 819–831.

Bacmeister, C.M., Huang, R., Osso, L.A., Thornton, M.A., Conant, L., Chavez, A.R., Poleg-Polsky, A., Hughes, E.G., 2022. Motor learning drives dynamic patterns of intermittent myelination on learning-activated axons. Nat. Neurosci. 25, 1300–1313.

Barak, B., Zhang, Z., Liu, Y., Nir, A., Trangle, S.S., Ennis, M., Levandowski, K.M., Wang, D., Quast, K., Boulting, G.L., Li, Y., Bayarsaihan, D., He, Z., Feng, G., 2019. Neuronal deletion of Gtf2i, associated with Williams syndrome, causes behavioral and myelin alterations rescuable by a remyelinating drug. Nat. Neurosci. 22, 700–708.

Blackmore, S., Hernandez, J., Juda, M., Ryder, E., Freund, G.G., Johnson, R.W., Steelman, A.J., 2017. Influenza infection triggers disease in a genetic model of experimental autoimmune encephalomyelitis. Proc. Natl. Acad. Sci. U.S.A. 114, E6107–e6116.

Camara, M.L., Corrigan, F., Jaehne, E.J., Jawahar, M.C., Anscomb, H., Baune, B.T., 2015. Effects of centrally administered etanercept on behavior, microglia, and astrocytes in mice following a peripheral immune challenge. Neuropsychopharmacology 40, 502–512.

Cameron, W., Doyle, K., Rocklin, R.E., 1986. Histamine type I (H1) receptor radioligand binding studies on normal T cell subsets, B cells, and monocytes. J. Immunol. (136), 2116–2120.

Centers for Disease Control and Prevention, National Center for Immunization and Respiratory Diseases.

Cervantes, O., Cruz Talavera, I., Every, E., Coler, B., Li, M., Li, A., Li, H., Adams Waldorf, K., 2022. Role of hormones in the pregnancy and sex-specific outcomes to infections with respiratory viruses. Immunol. Rev. 308, 123–148.

Chamberlain, K.A., Huang, N., Xie, Y., LiCausi, F., Li, S., Li, Y., Sheng, Z.H., 2021. Oligodendrocytes enhance axonal energy metabolism by deacetylation of mitochondrial proteins through transcellular delivery of SIRT2. Neuron 109, 3456–3472.e3458.

Chan, J.R., Watkins, T.A., Cosgaya, J.M., Zhang, C., Chen, L., Reichardt, L.F., Shooter, E. M., Barres, B.A., 2004. NGF controls axonal receptivity to myelination by Schwann cells or oligodendrocytes. Neuron 43, 183–191.

Chen, J.F., Liu, K., Hu, B., Li, R.R., Xin, W., Chen, H., Wang, F., Chen, L., Li, R.X., Ren, S. Y., Xiao, L., Chan, J.R., Mei, F., 2021a. Enhancing myelin renewal reverses cognitive dysfunction in a murine model of Alzheimer's disease. Neuron 109, 2292–2307 e2295.

Chen, J.F., Liu, K., Hu, B., Li, R.R., Xin, W., Chen, H., Wang, F., Chen, L., Li, R.X., Ren, S. Y., Xiao, L., Chan, J.R., Mei, F., 2021b. Enhancing myelin renewal reverses cognitive dysfunction in a murine model of Alzheimer's disease. Neuron 109, 2292–2307. e2295.

Chen, Y., Sheng, J., Tang, X., Zhao, Y., Zhu, S., Liu, Q., 2022. Clemastine rescues chemotherapy-induced cognitive impairment by improving white matter integrity. Neuroscience 484, 66–79.

Cordano, C., Sin, J.H., Timmons, G., Yiu, H.H., Stebbins, K., Guglielmetti, C., Cruz-Herranz, A., Xin, W., Lorrain, D., Chan, J.R., Green, A.J., 2022. Validating visual evoked potentials as a preclinical, quantitative biomarker for remyelination efficacy. Brain : J. Neurol. 145, 3943–3952.

Cree, B.A.C., Niu, J., Hoi, K.K., Zhao, C., Caganap, S.D., Henry, R.G., Dao, D.Q., Zollinger, D.R., Mei, F., Shen, Y.A., Franklin, R.J.M., Ullian, E.M., Xiao, L., Chan, J. R., Fancy, S.P.J., 2018. Clemastine rescues myelination defects and promotes functional recovery in hypoxic brain injury. Brain : J. Neurol. 141, 85–98.

DHooge, R., De Deyn, P.P., 2001. Applications of the Morris water maze in the study of learning and memory. Brain Res Brain Res Rev 36, 60–90.

Dawood, F.S., Iuliano, A.D., Reed, C., Meltzer, M.I., Shay, D.K., Cheng, P.Y., Bandaranayake, D., Breiman, R.F., Brooks, W.A., Buchy, P., Feikin, D.R., Fowler, K. B., Gordon, A., Hien, N.T., Horby, P., Huang, Q.S., Katz, M.A., Krishnan, A., Lal, R., Montgomery, J.M., Molbak, K., Pebody, R., Presanis, A.M., Razuri, H., Steens, A., Tinoco, Y.O., Wallinga, J., Yu, H., Vong, S., Bresee, J., Widdowson, M.A., 2012. Estimated global mortality associated with the first 12 months of 2009 pandemic influenza A H1N1 virus circulation: a modelling study. Lancet Infect. Dis. 12, 687–695.

Deacon, R.M., 2006. Burrowing in rodents: a sensitive method for detecting behavioral dysfunction. Nat. Protoc. 1, 118–121.

Deacon, R.M., Rawlins, J.N., 2005. Hippocampal lesions, species-typical behaviours and anxiety in mice. Behav. Brain Res. 156, 241–249.

Deacon, R.M., Raley, J.M., Perry, V.H., Rawlins, J.N., 2001. Burrowing into prion disease. Neuroreport 12, 2053–2057.

Deshmukh, V.A., Tardif, V., Lyssiotis, C.A., Green, C.C., Kerman, B., Kim, H.J., Padmanabhan, K., Swoboda, J.G., Ahmad, I., Kondo, T., Gage, F.H.,

Theofilopoulos, A.N., Lawson, B.R., Schultz, P.G., Lairson, L.L., 2013. A regenerative approach to the treatment of multiple sclerosis. Nature 502, 327–332.
Ekstrand, J.J., 2012. Neurologic complications of influenza. Semin. Pediatr. Neurol. 19, 96–100.
Fernandez-Castaneda, A., Lu, P., Geraghty, A.C., Song, E., Lee, M.H., Wood, J., O'Dea, M. R., Dutton, S., Shamardani, K., Nwangwu, K., Mancusi, R., Yalcin, B., Taylor, K.R., Acosta-Alvarez, L., Malacon, K., Keough, M.B., Ni, L., Woo, P.J., Contreras-Esquivel, D., Toland, A.M.S., Gehlhausen, J.R., Klein, J., Takahashi, T., Silva, J., Israelow, B., Lucas, C., Mao, T., Pena-Hernandez, M.A., Tabachnikova, A., Homer, R. J., Tabacof, L., Tosto-Mancuso, J., Breyman, E., Kontorovich, A., McCarthy, D., Quezado, M., Vogel, H., Hefti, M.M., Perl, D.P., Liddelow, S., Folkerth, R., Putrino, D., Nath, A., Iwasaki, A., Monje, M., 2022. Mild respiratory COVID can cause multi-lineage neural cell and myelin dysregulation. Cell 185, 2452–2468 e2416.
Fink, A.L., Engle, K., Ursin, R.L., Tang, W.Y., Klein, S.L., 2018. Biological sex affects vaccine efficacy and protection against influenza in mice. Proc. Natl. Acad. Sci. U.S. A. 115, 12477–12482.
Fünfschilling, U., Supplie, L.M., Mahad, D., Boretius, S., Saab, A.S., Edgar, J., Brinkmann, B.G., Kassmann, C.M., Tzvetanova, I.D., Möbius, W., Diaz, F., Meijer, D., Suter, U., Hamprecht, B., Sereda, M.W., Moraes, C.T., Frahm, J., Goebbels, S., Nave, K.A., 2012. Glycolytic oligodendrocytes maintain myelin and long-term axonal integrity. Nature 485, 517–521.
Graham, E.L., Clark, J.R., Orban, Z.S., Lim, P.H., Szymanski, A.L., Taylor, C., DiBiase, R. M., Jia, D.T., Balabanov, R., Ho, S.U., Batra, A., Liotta, E.M., Koralnik, I.J., 2021. Persistent neurologic symptoms and cognitive dysfunction in non-hospitalized Covid-19 "long haulers". Annals of clinical and translational neurology 8, 1073–1085.
Gwaltney Jr., J.M., Park, J., Paul, R.A., Edelman, D.A., O'Connor, R.R., Turner, R.B., 1996. Randomized controlled trial of clemastine fumarate for treatment of experimental rhinovirus colds. Clin. Infect. Dis. 22, 656–662.
Halder, N., Lal, G., 2021. Cholinergic system and its therapeutic importance in inflammation and autoimmunity. Front. Immunol. 12, 660342.
Heneka, M.T., Kummer, M.P., Latz, E., 2014. Innate immune activation in neurodegenerative disease. Nat. Rev. Immunol. 14, 463–477.
Hosseini, S., Wilk, E., Michaelsen-Preusse, K., Gerhauser, I., Baumgärtner, W., Geffers, R., Schughart, K., Korte, M., 2018. Long-term neuroinflammation induced by influenza A virus infection and the impact on hippocampal neuron morphology and function. J. Neurosci. : the official journal of the Society for Neuroscience 38, 3060–3080.
Jang, H., Boltz, D., Sturm-Ramirez, K., Shepherd, K.R., Jiao, Y., Webster, R., Smeyne, R. J., 2009. Highly pathogenic H5N1 influenza virus can enter the central nervous system and induce neuroinflammation and neurodegeneration. Proc. Natl. Acad. Sci. U.S.A. 106, 14063–14068.
Jang, H., Boltz, D., McClaren, J., Pani, A.K., Smeyne, M., Korff, A., Webster, R., Smeyne, R.J., 2012. Inflammatory effects of highly pathogenic H5N1 influenza virus infection in the CNS of mice. J. Neurosci. 32, 1545–1559.
Jelliffe, S.E., 1919. Nervous and mental disturbances of influenza. J. Nerv. Ment. Dis. 50, 405–407.
Johansen, P., Weiss, A., Bünter, A., Waeckerle-Men, Y., Fettelschoss, A., Odermatt, B., Kündig, T.M., 2011. Clemastine causes immune suppression through inhibition of extracellular signal-regulated kinase-dependent proinflammatory cytokines. J. Allergy Clin. Immunol. 128, 1286–1294.
Jurgens, H.A., Amancherla, K., Johnson, R.W., 2012. Influenza infection induces neuroinflammation, alters hippocampal neuron morphology, and impairs cognition in adult mice. J. Neurosci. : the official journal of the Society for Neuroscience 32, 3958–3968.
Klein, S.L., Hodgson, A., Robinson, D.P., 2012. Mechanisms of sex disparities in influenza pathogenesis. J. Leukoc. Biol. 92, 67–73.
Korte, M., Schmitz, D., 2016. Cellular and system biology of memory: timing, molecules, and beyond. Physiol. Rev. 96, 647–693.
Krementsov, D.N., Case, L.K., Dienz, O., Raza, A., Fang, Q., Ather, J.L., Poynter, M.E., Boyson, J.E., Bunn, J.Y., Teuscher, C., 2017. Genetic variation in chromosome Y regulates susceptibility to influenza A virus infection. Proc. Natl. Acad. Sci. U.S.A. 114, 3491–3496.
Li, Z., He, Y., Fan, S., Sun, B., 2015. Clemastine rescues behavioral changes and enhances remyelination in the cuprizone mouse model of demyelination. Neurosci. Bull. 31, 617–625.
Liu, J., Dupree, J.L., Gacias, M., Frawley, R., Sikder, T., Naik, P., Casaccia, P., 2016. Clemastine enhances myelination in the prefrontal cortex and rescues behavioral changes in socially isolated mice. J. Neurosci. : the official journal of the Society for Neuroscience 36, 957–962.
Lorenzo, M.E., Hodgson, A., Robinson, D.P., Kaplan, J.B., Pekosz, A., Klein, S.L., 2011. Antibody responses and cross protection against lethal influenza A viruses differ between the sexes in C57BL/6 mice. Vaccine 29, 9246–9255.
Lossos, A., Elazar, N., Lerer, I., Schueler-Furman, O., Fellig, Y., Glick, B., Zimmerman, B. E., Azulay, H., Dotan, S., Goldberg, S., Gomori, J.M., Ponger, P., Newman, J.P., Marreed, H., Steck, A.J., Schaeren-Wiemers, N., Mor, N., Harel, M., Geiger, T., Eshed-Eisenbach, Y., Meiner, V., Peles, E., 2015. Myelin-associated glycoprotein gene mutation causes Pelizaeus-Merzbacher disease-like disorder. Brain : J. Neurol. 138, 2521–2536.
Louie, A.Y., Tingling, J., Dray, E., Hussain, J., McKim, D.B., Swanson, K.S., Steelman, A. J., 2022. Dietary cholesterol causes inflammatory imbalance and exacerbates morbidity in mice infected with influenza A virus. J. Immunol. (208), 2523–2539.
Louie, A.Y., Kim, J.S., Drnevich, J., Dibaeinia, P., Koito, H., Sinha, S., McKim, D.B., Soto-Diaz, K., Nowak, R.A., Das, A., Steelman, A.J., 2023. Influenza A virus infection disrupts oligodendrocyte homeostasis and alters the myelin lipidome in the adult mouse. J. Neuroinflammation 20, 190.
Matty, M.A., Knudsen, D.R., Walton, E.M., Beerman, R.W., Cronan, M.R., Pyle, C.J., Hernandez, R.E., Tobin, D.M., 2019. Potentiation of P2RX7 as a host-directed strategy for control of mycobacterial infection. Elife 8.
Maurizi, C.P., 2010. Influenza caused epidemic encephalitis (encephalitis lethargica): the circumstantial evidence and a challenge to the nonbelievers. Med. Hypotheses 74, 798–801.
McKenzie, I.A., Ohayon, D., Li, H., de Faria, J.P., Emery, B., Tohyama, K., Richardson, W. D., 2014. Motor skill learning requires active central myelination. Science (New York, N.Y.) 346, 318–322.
Mei, F., Fancy, S.P.J., Shen, Y.A., Niu, J., Zhao, C., Presley, B., Miao, E., Lee, S., Mayoral, S.R., Redmond, S.A., Etxeberria, A., Xiao, L., Franklin, R.J.M., Green, A., Hauser, S.L., Chan, J.R., 2014. Micropillar arrays as a high-throughput screening platform for therapeutics in multiple sclerosis. Nat. Med. 20, 954–960.
Meyer, N., Richter, N., Fan, Z., Siemonsmeier, G., Pivneva, T., Jordan, P., Steinhäuser, C., Semtner, M., Nolte, C., Kettenmann, H., 2018. Oligodendrocytes in the mouse corpus callosum maintain axonal function by delivery of glucose. Cell Rep. 22, 2383–2394.
Oluich, L.J., Stratton, J.A., Xing, Y.L., Ng, S.W., Cate, H.S., Sah, P., Windels, F., Kilpatrick, T.J., Merson, T.D., 2012. Targeted ablation of oligodendrocytes induces axonal pathology independent of overt demyelination. J. Neurosci. : the official journal of the Society for Neuroscience 32, 8317–8330.
Pan, S., Mayoral, S.R., Choi, H.S., Chan, J.R., Kheirbek, M.A., 2020. Preservation of a remote fear memory requires new myelin formation. Nat. Neurosci. 23, 487–499.
Quarles, R.H., 2007. Myelin-associated glycoprotein (MAG): past, present and beyond. J. Neurochem. 100, 1431–1448.
Raison, C.L., Capuron, L., Miller, A.H., 2006. Cytokines sing the blues: inflammation and the pathogenesis of depression. Trends Immunol. 27, 24–31.
Ravenholt, R.T., Foege, W.H., 1982. 1918 influenza, encephalitis lethargica, parkinsonism. Lancet (London, England) 2, 860–864.
Riazi, K., Galic, M.A., Kentner, A.C., Reid, A.Y., Sharkey, K.A., Pittman, Q.J., 2015. Microglia-dependent alteration of glutamatergic synaptic transmission and plasticity in the hippocampus during peripheral inflammation. J. Neurosci. 35, 4942–4952.
Roda, R.H., FitzGibbon, E.J., Boucekkine, H., Schindler, A.B., Blackstone, C., 2016. Neurologic syndrome associated with homozygous mutation at MAG sialic acid binding site. Annals of clinical and translational neurology 3, 650–654.
Sabikunnahar, B., Lahue, K.G., Asarian, L., Fang, Q., McGill, M.M., Haynes, L., Teuscher, C., Krementsov, D.N., 2022. Sex differences in susceptibility to influenza A virus infection depend on host genotype. PLoS One 17, e0273050.
Schenk, F., Morris, R.G., 1985. Dissociation between components of spatial memory in rats after recovery from the effects of retrohippocampal lesions. Exp. Brain Res. 58, 11–28.
Schlesinger, R.W., Husak, P.J., Bradshaw, G.L., Panayotov, P.P., 1998. Mechanisms involved in natural and experimental neuropathogenicity of influenza viruses: evidence and speculation. Adv. Virus Res. 50, 289–379.
Shimizu, T., Nayar, S.G., Swire, M., Jiang, Y., Grist, M., Kaller, M., Sampaio Baptista, C., Bannerman, D.M., Johansen-Berg, H., Ogasawara, K., Tohyama, K., Li, H., Richardson, W.D., 2023. Oligodendrocyte dynamics dictate cognitive performance outcomes of working memory training in mice. Nat. Commun. 14, 6499.
Steadman, P.E., Xia, F., Ahmed, M., Mocle, A.J., Penning, A.R.A., Geraghty, A.C., Steenland, H.W., Monje, M., Josselyn, S.A., Frankland, P.W., 2020. Disruption of oligodendrogenesis impairs memory consolidation in adult mice. Neuron 105, 150–164.e156.
Surana, P., Tang, S., McDougall, M., Tong, C.Y., Menson, E., Lim, M., 2011. Neurological complications of pandemic influenza A H1N1 2009 infection: European case series and review. Eur. J. Pediatr. 170, 1007–1015.
Thaweethai, T., Jolley, S.E., Karlson, E.W., Levitan, E.B., Levy, B., McComsey, G.A., McCorkell, L., Nadkarni, G.N., Parthasarathy, S., Singh, U., Walker, T.A., Selvaggi, C. A., Shinnick, D.J., Schulte, C.C.M., Atchley-Challenner, R., Alba, G.A., Alicic, R., Altman, N., Anglin, K., Argueta, U., Ashktorab, H., Baslet, G., Bassett, I.V., Bateman, L., Bedi, B., Bhattacharyya, S., Bind, M.A., Blomkalns, A.L., Bonilla, H., Bush, P.A., Castro, M., Chan, J., Charney, A.W., Chen, P., Chibnik, L.B., Chu, H.Y., Clifton, R.G., Costantine, M.M., Cribbs, S.K., Davila Nieves, S.I., Deeks, S.G., Duven, A., Emery, I.F., Erdmann, N., Erlandson, K.M., Ernst, K.C., Farah-Abraham, R., Farner, C.E., Feuerriegel, E.M., Fleurimont, J., Fonseca, V., Franko, N., Gainer, V., Gander, J.C., Gardner, E.M., Geng, L.N., Gibson, K.S., Go, M., Goldman, J. D., Grebe, H., Greenway, F.L., Habli, M., Hafner, J., Han, J.E., Hanson, K.A., Heath, J., Hernandez, C., Hess, R., Hodder, S.L., Hoffman, M.K., Hoover, S.E., Huang, B., Hughes, B.L., Jagannathan, P., John, J., Jordan, M.R., Katz, S.D., Kaufman, E.S., Kelly, J.D., Kelly, S.W., Kemp, M.M., Kirwan, J.P., Klein, J.D., Knox, K.S., Krishnan, J.A., Kumar, A., Laiyemo, A.O., Lambert, A.A., Lanca, M., Lee-Iannotti, J.K., Logarbo, B.P., Longo, M.T., Luciano, C.A., Lutrick, K., Maley, J.H., Marathe, J.G., Marconi, V., Marshall, G.D., Martin, C.F., Matusov, Y., Mehari, A., Mendez-Figueroa, H., Mermelstein, R., Metz, T.D., Morse, R., Mosier, J., Mouchati, C., Mullington, J., Murphy, S.N., Neuman, R.B., Nikolich, J.Z., Ofotokun, I., Ojemakinde, E., Palatnik, A., Palomares, K., Parimon, T., Parry, S., Patterson, J.E., Patterson, T.F., Patzer, R.E., Peluso, M.J., Pemu, P., Pettker, C.M., Plunkett, B.A., Pogreba-Brown, K., Poppas, A., Quigley, J.G., Reddy, U., Reece, R., Reeder, H., Reeves, W.B., Reiman, E.M., Rischard, F., Rosand, J., Rouse, D.J., Ruff, A., Saade, G., Sandoval, G.J., Schlater, S.M., Shepherd, F., Sherif, Z.A., Simhan, H., Singer, N.G., Skupski, D.W., Sowles, A., Sparks, J.A., Sukhera, F.I., Taylor, B.S., Teunis, L., Thomas, R.J., Thorp, J.M., Thuluvath, P., Ticotsky, A., Tita, A.T., Tuttle, K.R., Urdaneta, A.E., Valdivieso, D., VanWagoner, T.M., Vasey, A., Verduzco-Gutierrez, M., Wallace, Z.S., Ward, H.D., Warren, D.E., Weiner, S.J., Welch, S., Whiteheart, S.W., Wiley, Z., Wisnivesky, J.P., Yee, L.M., Zisis, S., Horwitz, L.I., Foulkes, A.S., 2023. Development of a definition of postacute sequelae of SARS-CoV-2 infection. JAMA 329, 1934–1946.

Thomson, C.A., McColl, A., Cavanagh, J., Graham, G.J., 2014. Peripheral inflammation is associated with remote global gene expression changes in the brain. J. Neuroinflammation 11, 73.
Turner, R.B., Sperber, S.J., Sorrentino, J.V., O'Connor, R.R., Rogers, J., Batouli, A.R., Gwaltney Jr., J.M., 1997. Effectiveness of clemastine fumarate for treatment of rhinorrhea and sneezing associated with the common cold. Clin. Infect. Dis. 25, 824–830.
Vitkovic, L., Konsman, J.P., Bockaert, J., Dantzer, R., Homburger, V., Jacque, C., 2000. Cytokine signals propagate through the brain. Mol. Psychiatr. 5, 604–615.
Volk, P., Rahmani Manesh, M., Warren, M.E., Besko, K., Gonçalves de Andrade, E., Wicki-Stordeur, L.E., Swayne, L.A., 2023. Long-term neurological dysfunction associated with COVID-19: lessons from influenza and inflammatory diseases? J. Neurochem.
Vorhees, C.V., Williams, M.T., 2006. Morris water maze: procedures for assessing spatial and related forms of learning and memory. Nat. Protoc. 1, 848–858.
Wang, G.F., Li, W., Li, K., 2010. Acute encephalopathy and encephalitis caused by influenza virus infection. Curr. Opin. Neurol. 23, 305–311.
World Health Organization. Burden of Disease.
Xu, E., Xie, Y., Al-Aly, Z., 2022. Long-term neurologic outcomes of COVID-19. Nat. Med. 28, 2406–2415.
Zhu, T.T., Wang, H., Liu, P.M., Gu, H.W., Pan, W.T., Zhao, M.M., Hashimoto, K., Yang, J. J., 2024. Clemastine-induced enhancement of hippocampal myelination alleviates memory impairment in mice with chronic pain. Neurobiol. Dis. 190, 106375.